Appl. Phys. B 73, 401–406 (2001)
DOI: 10.1007/s003400100654

Applied Physics B
Lasers and Optics

P.-G. REINHARD[1]
E. SURAUD[2]

Dynamics of Na clusters in picosecond laser pulses

[1] Institut für Theoretische Physik, Universität Erlangen, Staudtstrasse 7, 91058 Erlangen, Germany
[2] Laboratoire de Physique Quantique, Université Paul Sabatier, 118 Route de Narbonne, 31062 Toulouse Cedex, France

Received: 3 July 2001
Published online: 10 October 2001 •

ABSTRACT We investigate the electronic and ionic dynamics of Na clusters under the influence of a laser pulse in the range 100 femtoseconds to picoseconds. The dynamics is described by means of the time-dependent local-density approximation coupled to ionic molecular dynamics (TDLDA-MD). Variation of pulse length allows us to explore the time scales of ionic motion in a manner similar to pump and probe experiments. Resonant enhancement of electron emission serves as a measure for the time scale of Coulomb explosion.

PACS 36.40.Gk; 36.40.Qv; 36.40.Wa

1 Introduction

Clusters exposed to short laser pulses display a variety of interesting dynamical phenomena. Very strong pulses trigger a straightforward Coulomb explosion [1], which can proceed in a remarkably violent fashion if an appropriately reactive material is chosen [2]. Equally interesting are intermediate strengths combined with the tunable time profile of the laser. These allow us to get an insight into the coupled electronic and ionic dynamics of clusters, as demonstrated in the experiments of [3]. Two effects can be seen there: first, the release of core electrons if the cluster has reached a critical ionic distance during its Coulomb expansion and, second, a plasmon-enhanced ionization if the growing cluster radius brings the Mie surface plasmon into resonance with the laser field. The first process dominates at larger laser intensities and the second at lower intensities. The critical intensity is reached when the laser field just compensates the cluster-binding forces [4]. Both regimes are accessed by the experiments. A theoretical description in the regime of intense fields can employ classical concepts with a little quantum information about the core electrons [5]. The regime of sub-critical (but still strong) fields is accessible to a detailed quantum-mechanical description at the level of the time-dependent local-density approximation (TDLDA) for the electrons coupled to simultaneous ionic molecular dynamics (MD). A first discussion of plasmon-enhanced ionization during Coulomb expansion on the grounds of TDLDA-MD was published in [6]. It is the aim of the present paper to continue these studies in a more detailed way. Thereby we pay particular attention to systematic trends with laser intensity and pulse length, in a manner similar to what has been done in the experimental analysis [3]. As in our previous studies [6], we take Na clusters as test cases. This means that we concentrate on the resonant effects in the shell of valence electrons. The excitation of core electrons can be neglected for Na clusters in the regime of sub-critical laser fields, and that is the working regime of the present studies.

2 Framework

The TDLDA-MD has been presented in detail previously, see e.g. the review article [7]. We briefly sketch here the essential ingredients for the actual case. The electrons are treated in the time-dependent local-density approximation employing the exchange correlation functional of [8]. The ions follow classical molecular dynamics under the influence of the mutual repulsion between the ions and the force coming from the electrons. Only the valence electrons are treated. A local pseudo-potential is used to describe the coupling of valence electrons and ions [9]. The pseudo-potential is tuned to deliver also a good description of optical response. The handling of the electrons is simplified by using cylindrically averaged potentials, which gives a fair approximation for clusters with nearly spherical or axial shape [10]. Our test cases Na_9^+ and Na_{41}^+ are close to spherical and thus well adapted to the cylindrical approximation.

Before proceeding to the violent cluster dynamics, it is worthwhile to recall the spectral properties of our main test case Na_9^+. The ionic configuration consists of two rings of four ions each, followed by a single ion at the top. The axis from the top ion through the centers of the two rings is the symmetry axis, called the z-axis. The laser couples dominantly to the dipole modes and we shall polarize the laser along the above-defined z-axis. Figure 1 shows the spectral distribution in the dipole channel along the z-axis. One sees the dramatic dominance of the Mie surface-plasmon peak at 2.7 eV. The strength is, in fact, slightly fragmented by interference with a $1ph$ state that lies close-by. This double-peak structure of the plasmon resonance is in accordance with the experimental findings [11]. There are several fur-

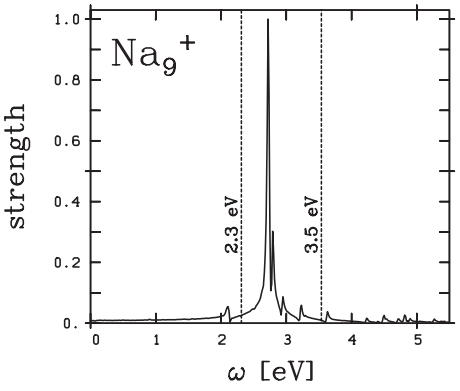

FIGURE 1 The dipole power spectrum of Na_9^+. The *vertical dotted lines* indicate the two laser frequencies which will be considered in the following

ther minor peaks, most of them above resonance where the density of states naturally increases. It is to be remarked that the position of the Mie surface plasmon depends sensitively on the global geometry of the cluster. The larger the extension in the z-direction, the lower the resonance frequency, and vice versa. In turn, a change of the cluster radius R scales the resonance frequency as $R^{-3/2}$, while a change of quadrupole deformation β_2 leads to a splitting of the resonance: the mode in the elongated direction is lowered and the mode in the compressed direction is shifted to higher frequencies. Last but not least, the net charge has a strong influence. Increasing the net charge increases the plasmon frequency. For a more detailed discussion and examples of these dependences see e.g. [12]. All these global properties of the optical response can change substantially in the course of cluster dynamics under strong laser fields. It is thus desirable to have a simple estimate for the actual position of the surface-plasmon resonance. We have computed the dipole spectrum for a Na cluster with $N_{\rm ion} = 9$ on a grid of various radii, deformations, and charge states. From that we have fitted the following re-scaling formula for the resonance mode in the z-direction:

$$\frac{\omega(R,\beta,N_{\rm el})}{\omega_0} = \frac{R}{R_0}\left(1+\frac{N_{\rm ion}-N_{\rm el}-1}{70}\right)(1-0.3\,\beta_2)\,, \qquad (1)$$

where $\omega_0 = 2.7$ eV is the plasmon frequency of the initial Na_9^+ cluster and R_0 its radius. Mind that this estimate characterizes the average resonance position. The width generally increases in the course of the dynamics. It depends on the detailed history of the process and cannot be parameterized as easily.

Figure 1 also indicates by vertical lines the two laser frequencies which we will discuss in the following, one below and the other above the resonance. The lower frequency corresponds to the test case of [3]. It is best suited for exploring the Coulomb expansion. The plasmon frequency goes down with increasing radius, see (1). Thus the plasmon moves into resonance with the laser pulse at a certain time of the dynamical evolution. This leads to a sensitive dependence of the dynamics on the temporal profile of the laser. As a second test case, we also consider a laser pulse with a frequency above the plasmon resonance. This test case accesses only the higher-lying peaks with smaller strengths and thus we expect similar but less dramatic trends.

3 Results and discussion

3.1 *Basic scenario*

The experiments of [3] were performed with laser pulses of variable length in the range from 100 femtoseconds to a few picoseconds. The dynamical effects were analyzed by varying the pulse length and looking at the output in terms of ionization and the various fragments. As observed from our former calculations [6], a simpler 'theoretical' solution consists in investigating the dynamics by using a continuous laser pulse and tracing the subsequent dynamical observable (ionization, ionic motion) as a function of time. The effect of a pulse with given length $T_{\rm pulse}$ can be read off approximately from the status of the observable at this time. The ionization changes less than 10% once a pulse has been switched off. Thus the net ionization can be estimated that way within 10% and the critical ionic radii even more precisely. This precision suffices for the present studies and the approximation to use one pulse per intensity (and frequency) reduces the expense dramatically. A little care has to be taken when switching on the laser. a sufficiently smooth switching is required to guarantee a well-defined frequency. We mostly use here a sine-ramp with length 10 fs. All test cases work in a range of laser intensities of 10^{10}–10^{12} W/cm^2. This is far below the critical intensity of 10^{14} W/cm^2 where resonant mechanisms are overridden by direct field emission [4] and where core electrons are released [5]. The presently used moderate intensities are thus ideally suited to explore resonant mechanisms.

3.2 *The critical role of laser intensity*

Figure 2 shows a series of results for the lower laser frequency ($\omega_{\rm las} = 2.3$ eV) and varying laser intensity. The evolution of ionization can be read off from the uppermost panel (ionization state is $N_{\rm esc}+1$). The range of intensities is chosen such that the lowest intensity I_0 has little effect, the cluster acquiring just one extra charge after a long pulse. Ionization increases dramatically with intensity [13] and thus we see in a few small intensity steps the sudden transition to full ionization within less than a picosecond. That stage is reached shortly above $I = 2I_0$. Further increase of intensity reduces the time scale for full ionization. This is thus also the range of intensities where the resulting ionization depends sensitively on time, i.e. on the laser pulse length $T_{\rm pulse}$: the two curves with lower intensity ($I < 2I_0$) increase steadily while the time evolutions of $N_{\rm esc}$ for the three higher intensities ($I > 2I_0$) all show a short time interval with a very high slope. An enhanced emission is taking place here. This time of enhanced emission is correlated to a time of large dipole response (not shown here). And, such enhanced dipole amplitude is a unique signal of resonant response. The reason for that enhanced response is seen from the lowest panel of Fig. 2. The initial ionization drives a Coulomb expansion of the cluster. The increasing cluster radius will bring the surface plasmon into resonance with the laser at some time. The strong slopes in $N_{\rm esc}$ are correlated with a r.m.s. ionic radius of about $8a_0$, which corresponds to a radius growth of about 25% as compared to ground-state radius. A complementing view is given in the middle panel where we show the time evolution of the average plasmon frequency estimated according to (1). The sequence of intersections with the laser frequency (horizontal straight

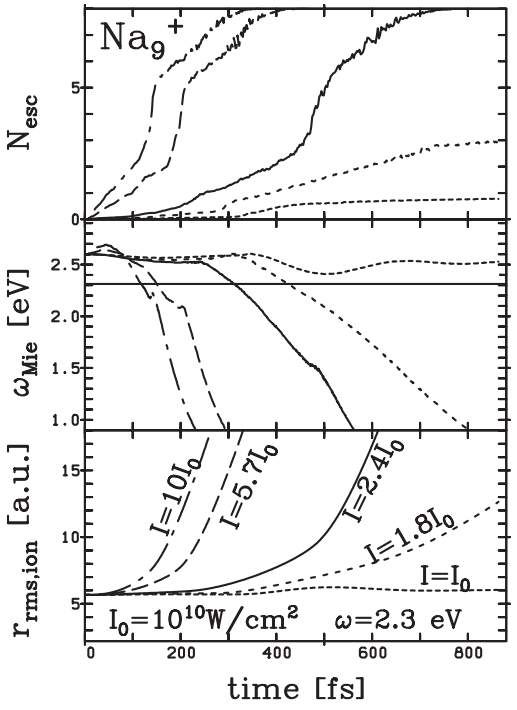

FIGURE 2 Time evolution of key observables for Na_9^+ irradiated by laser pulses with varying intensity as indicated. All pulses have frequency $\omega = 2.3$ eV and a pulse length of 1000 fs. *Lowest panel*: ionic r.m.s. radius. *Middle panel*: frequency of the average Mie plasmon peak; the *horizontal straight line* indicates the laser frequency. *Uppermost panel*: number of emitted electrons $N_{\rm esc}$

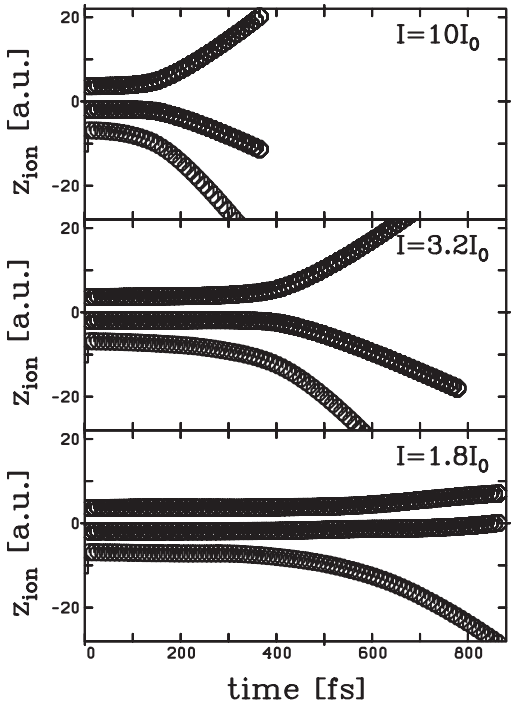

FIGURE 3 Time evolution of the nine ionic z-coordinates in Na_9^+ for three selected laser intensities as indicated

line) agrees with the sequence of resonant slopes. The actual times deviate a little for the case of $2.4I_0$. But mind that we are using a simple estimate of the plasmon frequency from near-to-ground-state calculations while the electron cloud is actually far from equilibrium. At least the trends are reproduced correctly: larger intensity produces larger initial (off-resonant) ionization. This leads to faster Coulomb expansion which, in turn, reaches more quickly the resonance conditions. a too-low intensity never reaches the critical point.

There is also a jump from moderate Coulomb expansion in the sub-critical regime to a straightforward Coulomb explosion after resonance. It can be guessed from the slope of ionic radii in the lower panel of Fig. 2. A more direct view is given in Fig. 3, where we show the evolution of the detailed ionic positions along the laser polarization axis. The lowest panel shows a sub-critical case of mere Coulomb expansion. In fact, we see that the positive net charge just pushes the top ion away from the residual, still fairly intact, cluster. The more violent cases demonstrate clearly the dissolution of the total cluster (mind that a similar explosion of the rings is seen in the x–y-plane, not shown here). The time scales seen here are the same as the time scales seen for the ionic radii in Fig. 2. The clock is set by the speed of initial ionization (determined by laser intensity) and by the time scale of ionic response. The latter takes typically 50–100 fs for Na clusters [7, 14]. Heavier materials will react more slowly and lighter ones faster.

3.3 *Fluence*

The upper panel of Fig. 2 can be viewed as final ionization versus pulse length for various intensities. It is customary to combine pulse length $T_{\rm pulse}$ and intensity I into fluence $IT_{\rm pulse}$. The fluence quantifies the total energy impact through the laser pulse, independent of its length. One can thus expect that results depend predominantly on the fluence and not so much on the detailed composition, in terms of intensity and pulse duration. Figure 4 shows ionization and ionic radii versus fluence $IT_{\rm pulse}$ for the same test cases as in Fig. 2. The patterns for the electronic observable $N_{\rm esc}$ now come much closer together. The three cases in the regime of resonant response coalesce almost to one curve. This shows that fluence is indeed an appropriate combination to characterize laser effects on electrons. The large differences between non-resonant and resonant regimes remain, of course, also visible in this presentation. But note that at least the early stages of purely electronic response coincide fairly well for all cases. The differences are driven mainly by the ionic response. For completeness the lower panel of Fig. 4 shows the evolution of ionic radii in terms of fluence. The patterns do not coalesce and stay as different as they were before, however, with exchanged ordering. Ionic motion carries its own time scale of about 50 fs (for the onset of ionic motion) to 300 fs (for one ionic oscillation). This time scale can then hardly be directly influenced by laser conditions. Thus it interferes with a sorting in terms of fluence.

Up to now, all figures have shown the detailed evolution in the various test cases. What counts at the end are more global results as e.g. the final ionization. Such a summarized view is given in Fig. 5. We have looked for the time at which ionization stage 6 ($\equiv N_{\rm esc} = 5$) is reached for each different intensity. The resulting critical time for this event is drawn versus intensity in the lower panel. The trend is obvious: the lower the intensity the longer irradiation time needed and the trend resembles a $1/I$ behavior. As complementing informa-

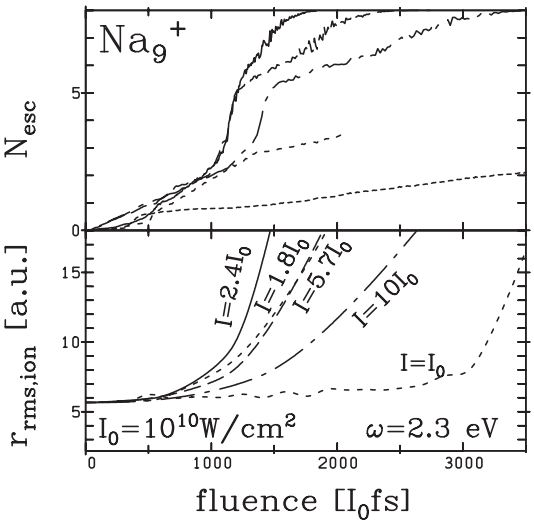

FIGURE 4 Same as Fig. 2 but drawn versus fluence $T_{\rm pulse} I_0$ rather than versus time t itself

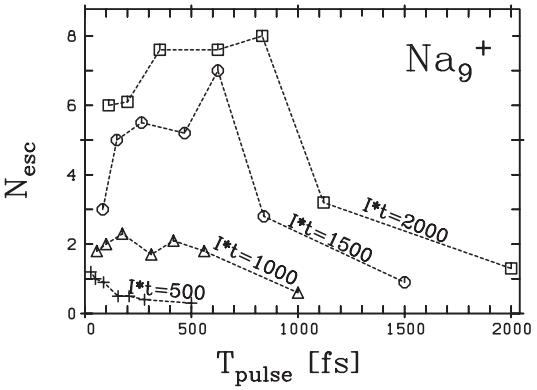

FIGURE 6 Final number of emitted electrons versus length of laser pulse $T_{\rm pulse}$ for lasers with frequency $\omega = 2.3$ eV and different fluences $IT_{\rm pulse}$. Results of lasers with the same fluence are connected by *lines* and denoted by using the same *symbol*. The fluence is given in units of I_0 fs, where $I_0 = 10^{10}$ W/cm^2. Test case is $Na_9{}^+$

tion, we have evaluated the time at which the plasmon comes into resonance with the laser. The resulting curve has a very similar pattern. These trends suggest that results in terms of fluence $It_{\rm crit}$ should become independent of intensity. This aspect is shown in the upper panel of Fig. 5. We find indeed that the fluence needed to reach ionization stage 6 is only weakly dependent on the intensity. The curve has an abrupt turn at lower intensity, where time and fluence to reach resonant conditions jump to very large values because a different dynamical scenario comes into play. The example nevertheless shows that fluence can indeed provide a more robust measure for the laser input. It can achieve flat trends of observables in regions which follow the same dynamical scenario. But it does not hinder, of course, the sudden changes of results if the underlying dynamics undergoes dramatic changes, such as (in our example) the transition from steady ionization to resonant enhancement (see the kink at $I = 2I_0$ in Fig. 5).

Figure 6 shows a summary of results in the same manner as it was presented in [3], namely as ionization versus laser pulse length $T_{\rm pulse}$ at fixed fluence. And, the patterns here are much the same as in [3]. There is little ionization for long pulses because the field strength is too low to produce sufficient initial ionization. Lowering $T_{\rm pulse}$ enables the resonant mechanisms and yields a sudden increase in ionization. Pulse lengths below 100 fs are too short to await ionic response and thus have again lower ionization. The resonance peak is more pronounced for high fluence. Low fluences stay sub-critical at all times and thus yield a flat profile in the figure.

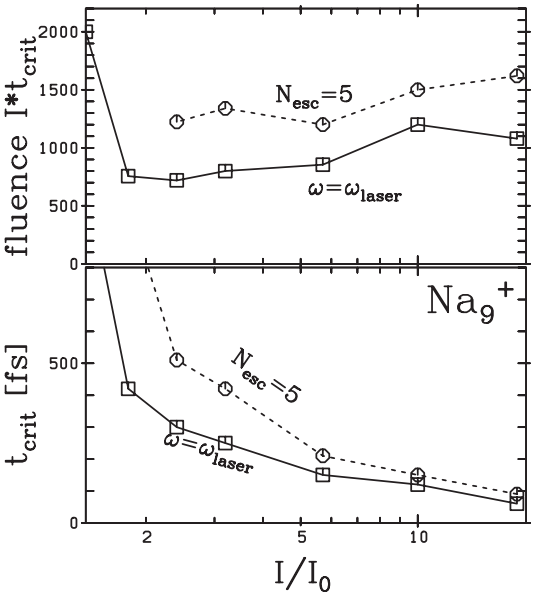

FIGURE 5 Laser pulse lengths $t_{\rm crit}$ to reach coincidence of Mie frequency with laser frequency (*full line, open squares*) or to reach an emission of five electrons (*dotted line, open circles*), again for the test case Na_9^+ irradiated by laser pulses with varying intensity (dependence on *horizontal axis*) and frequency $\omega = 2.3$ eV. The *upper panel* shows the same quantities in terms of fluence $t_{\rm crit} I/I_0$

3.4 *Exploring laser frequencies above resonance*

The case of a laser pulse above plasmon resonance is shown in Fig. 7. The time evolution for the various intensities look very similar to the previous case of lower frequency. The time scales for the onset of the strong slopes are typical ionic times. Thus we see again a resonant enhancement driven by ionic expansion. Still, the total ionization and the Coulomb expansion are not as dramatic as before. This hints that a less-pronounced state in the electronic spectrum is moved into resonance. The critical ionic r.m.s. radii where the strong slopes occur are here around $6.5a_0$, corresponding to only 12% expansion. This indicates that the state lies initially closer above the laser frequency. And indeed we see in the spectrum (Fig. 1) a small peak at about 3.7 eV, just a little above the laser frequency of 3.5 eV. The effects are less pronounced than they were in the case of the plasmon resonance. But this example together with a quick glance at the spectrum shows that it is almost impossible to find a true spectral vacuum above the plasmon resonance. Thus some resonantly enhanced ionization will be seen almost everywhere. However, a clear-cut analysis in these cases of secondary resonances is very hard because of the large density of excited states and their broad variety of intrinsic structures.

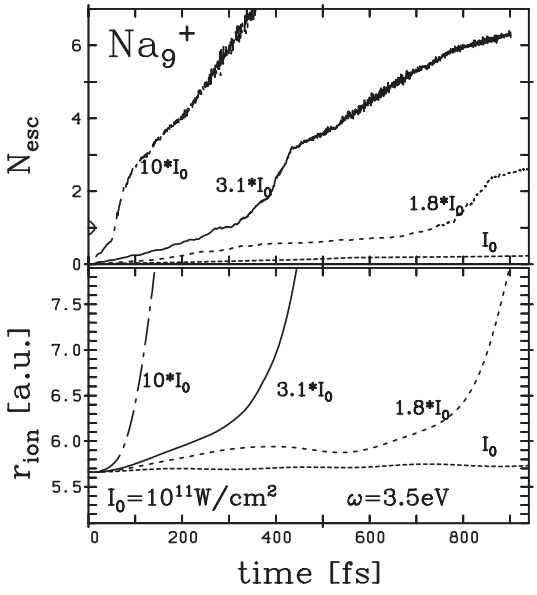

FIGURE 7 Time evolution of key observables for Na_9^+ irradiated by laser pulses with varying intensity as indicated. All pulses have frequency $\omega = 3.5$ eV and a pulse length of 1000 fs. *Lower panel*: ionic r.m.s. radius. *Upper panel*: number of emitted electrons $N_{\rm esc}$

In [6] we explored the role of pulse duration on ionization in the case of the bigger cluster Na_{41}^+ and found a double enhancement of ionization for frequencies somewhat above the surface-plasmon frequency. A first enhancement was of electronic nature due to the blue shift of the plasmon resonance (i.e. here the shift towards laser frequency) following early ionization. The plasmon frequency was then shooting above the laser frequency. The second enhancement was due to ionic expansion as discussed at length here. And we found that the time scale separating electron-enhanced and ion-enhanced emissions was around 200 fs, the typical time for ionic response. It is interesting to complement this study by exploring another range of frequencies, higher above resonance than before. We have chosen here two cases. The first case is at frequency 3.5 eV, as in Na_9^+, which again is a little below a small peak at about 3.6 eV in Na_{41}^+. The second case is chosen at 6 eV aiming at touching the (faint) volume plasmon. We are in both cases far away from marked resonances (similar to the previous case of Na_9^+ at 3.5 eV). Thus we need to scan a large range of intensities to observe sizable ionization. Results are displayed in Fig. 8. The lower panel shows the case at 6 eV. No resonance mechanism is at work here. Ionization increases steadily with intensity and with time. The case at 3.5 eV exhibits a slightly more complicated pattern. There is some resonance mechanism at work. The behavior is similar to Fig. 7 and we see probably again a weak resonant enhancement driven by expansion coinciding with a small side-peak shortly above the laser frequency. It is interesting to note that the larger cluster Na_{41}^+ still has no pronounced sub-structures in the high-frequency regime in spite of the expected higher-level density. One may even spot a hint of a double-resonant mechanism for the case at intensity $I = 66 I_0$.

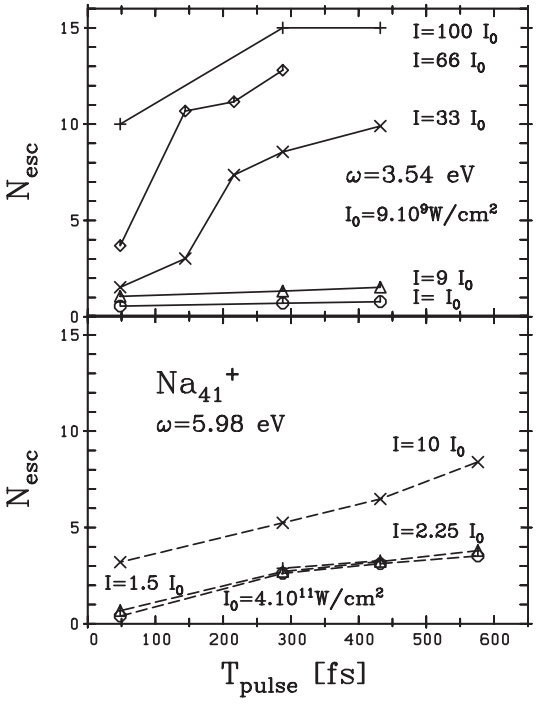

FIGURE 8 Final ionization as a function of pulse duration for two frequencies above resonance and at various intensities

3.5 *Scanning frequencies*

It is finally interesting to complement the results of Sect. 3.4 and of [6] by scanning a larger range of frequencies at fixed laser intensity. This is done in Fig. 9 again for Na_{41}^+. The frequencies are scanned in the low-intensity range ($I = 9 \times 10^9$ W cm^{-2}) of [6]. The patterns are here very clear. While the two cases close to the Mie plasmon (2.86 and 2.72 eV) exhibit a clear resonance regime with strongly enhanced slope, the two other cases out of resonance deliver essentially flat trends. The case above resonance ($\omega = 3.54$ eV) remains totally inert. The case below resonance ($\omega = 2.45$ eV) shows the onset of resonant enhancement towards the end of the observation time. This hints that lasers below the plasmon frequency may always reach a resonant regime at some time, i.e. given enough patience. Altogether the trends thus confirm our previous conclusions.

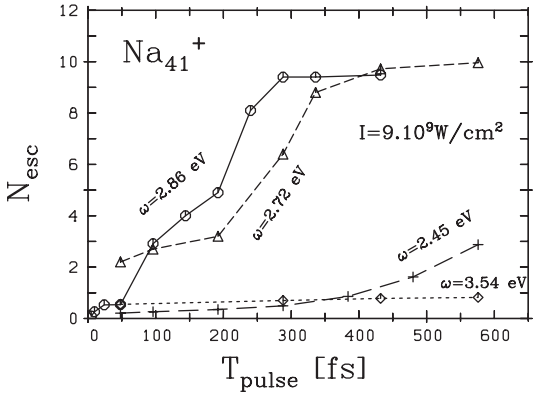

FIGURE 9 Final ionization as a function of pulse duration for various laser frequencies below and above plasmon resonance. The intensity is here fixed as indicated in the figure

4 Conclusions

Motivated by former experimental [3] and theoretical [6] analysis, we have explored in this paper the response of metal clusters under the influence of femto- to picosecond laser pulses at moderate intensities. We have investigated more systematically the resonant enhancement of ionization due to ionic expansion. Re-shuffling the trends in terms of laser fluence (rather than laser intensity) yields patterns with the same structure as seen experimentally [3]. Trends with fluence are usually weaker than trends with intensity as long as one stays in one regime with similar electronic dynamics and as long as one does not interfere too much with ionic time scales. The most pronounced resonant enhancement is seen for laser frequencies below the Mie surface plasmon, because this gives the plasmon the chance to come into resonance with laser in the course of the ionic expansion. But we see also resonant mechanisms for lasers above the plasmon frequency, because there are still sharp enough side-peaks in the vicinity above the plasmon. But all trends are flat far above the plasmon (about double-frequency and more). This is in the range of the electron continuum and there are no sufficiently pronounced states left over. The laser frequencies close to resonance exhibit interesting double electronic and ionic enhancement mechanisms. Tiny changes in frequencies switch very quickly from one dynamical regime to the next. This region deserves certainly even more systematic studies. We have focused here on laser intensities mostly leading to the explosion of the irradiated clusters. The case of still more moderate intensities is interesting as well, and actually gives access to crucial information on vibrational dynamics clusters. This is the regime of pump and probe experiments that are worth investigating systematically as well. Work along this line is in progress.

ACKNOWLEDGEMENTS The authors are grateful for the French–German exchange program PROCOPE No. 99 074 and thank the Institut Universitaire de France for financial support during the realization of this work.

REFERENCES

1 T. Ditmire, J.W.G. Tisch, E. Springate, M.B. Mason, N. Hay, R.A. Smith, J. Marangos, M.H.R. Hutchinson: Nature **386**, 54 (1997)
2 J. Zweiback, R.A. Smith, T.E. Cowan, G. Hays, K.B. Wharton, Y.P. Yanovski, T. Ditmire: Phys. Rev. Lett. **84**, 2634 (2000)
3 L. Köller, M. Schumacher, J. Koehn, S. Teuber, J. Tiggesbaeumker, K.-H. Meiwes-Broer: Phys. Rev. Lett. **82**, 3783 (1999)
4 P.-G. Reinhard, E. Suraud: Eur. Phys. J. D **3**, 175 (1998)
5 C. Siedschlag, J.M. Rost: preprint 2000
6 E. Suraud, P.-G. Reinhard: Phys. Rev. Lett. **85**, 2296 (2000)
7 F. Calvayrac, P.-G. Reinhard, E. Suraud, C. Ullrich: Phys. Rep. **337**, 493 (2000)
8 J.P. Perdew, Y. Wang: Phys. Rev. B **45**, 13 244 (1992)
9 S. Kümmel, M. Brack, P.-G. Reinhard: Eur. Phys. J. D **9**, 149 (1999)
10 B. Montag, P.-G. Reinhard: Z. Phys. **D33**, 265 (1995)
11 T. Reiners, C. Ellert, M. Schmidt, H. Haberland: Phys. Rev. Lett. **74**, 1558 (1997)
12 P.-G. Reinhard, O. Genzken, M. Brack: Ann. Phys. (Leipzig) **5**, 576 (1996)
13 C.A. Ullrich, P.-G. Reinhard, E. Suraud: J. Phys. B **30**, 5043 (1997)
14 P.-G. Reinhard, F. Calvayrac, C. Kohl, S. Kümmel, E. Suraud, C.A. Ullrich, M. Brack: Eur. Phys. J. D **9**, 111 (1999)